Exchange Interaction between Copper(II) Ions through Glutamic Acid Molecules

C. D. Brondino,[1a] N. M. C. Casado,[1a] M. C. G. Passeggi,[1b] and R. Calvo*,[1a,b]

Departamento de Física, Facultad de Bioquímica y Ciencias Biológicas (UNL), C.C.530, Ciudad Universitaria, 3000 Santa Fe, Argentina, and INTEC (CONICET-UNL), Güemes 3450, 3000 Santa Fe, Argentina

Received August 20, 1992

EPR measurements at ω_0 = 9.7 and 33.3 GHz microwave frequencies in single crystals of the copper complex of glutamic acid [Cu(glu)] and at 9.8 GHz in the zinc complex of glutamic acid [Zn(glu)] doped with ^{63}Cu have been performed at room temperature. A single EPR line was observed in Cu(glu) for any orientation of the magnetic field **B** at both frequencies. The gyromagnetic tensor exhibits axial symmetry, and the line width $\Delta B_{pp}(\theta,\phi)$ is strongly dependent on ω_0. We calculate the dependence of the line width with ω_0 in terms of the exchange interactions between the copper ions. This is achieved with a model based on Kubo and Tomita's theory, which allows us to evaluate selectively the exchange coupling constants $|J|$ between nonequivalent copper ions in the unit cell. Pathways for superexchange between copper ions in Cu(glu) are provided by carboxylate bridges and hydrogen bonds, as well as by glutamic acid units. From the data we estimate $|J_\sigma|$ = 0.19 K between copper ions in a distorted octahedral coordination, connected equatorially through the σ skeleton of a glutamic acid molecule. This bridge involves six diamagnetic atoms. A lower limit for the exchange parameter assigned to the carboxylate paths is estimated as $|J_c| > 1$ K. The results obtained for Zn(glu) doped with ^{63}Cu are used to study the electronic properties of the isolated copper ions, which in turn allow one to understand the overall axial symmetry of the $\mathbf{g}^2$ tensor, and the line width data obtained in Cu(glu).

Introduction

The magnetic properties of several copper amino acid complexes (CACS) have been studied in recent years using various experimental techniques.[2-8] The main purpose of those investigations was to evaluate the magnitudes of the exchange coupling parameters and to correlate their values with the characteristics of the chemical paths for superexchange. X-ray structural studies indicate that most CACS have copper ions in chains or layers. Then, they exhibit an interesting low-dimensional magnetic behavior observed through magnetic susceptibility,[2,4] electron paramagnetic resonance (EPR),[3,5,8] and specific heat measurements.[6,7] These compounds are also simple model systems that can be used to understand exchange interactions between metal ions or between metal ions and free radicals observed in more complex metalloproteins.[9,10] Since the typical magnitudes of the exchange couplings J involved in CACS are similar to those of the Zeeman energies, the EPR technique is particularly adequate for a magnetic characterization of these compounds. In fact, EPR data allow for obtaining values of $|J|$ within the range 0.001–1 K, in experiments performed in single crystals at room temperature.[3,5] Also, in some cases it is possible to evaluate exchange interactions between specific spins,[3d] instead of bulk mean values, such as those obtained from thermodynamic properties.

The best studied CACS are $Cu(aa)_2$, in which the copper ions are bonded to two amino acid molecules, either in octahedral or in square planar configurations. In most $Cu(aa)_2$, copper ions at about 5 Å are connected by carboxylate as well as by hydrogen-bond bridges, both paths being in principle able to transfer spin polarization. These bridges can provide the dominant pathways for superexchange depending on the case.[7,11]

In this paper we report an EPR study of electronic properties and magnetic interactions in single crystals of the dihydrated copper and zinc (doped with ^{63}Cu) complexes of glutamic acid (glu) [Me(glu) = $Me(CO_2(CH_2)_2CHNH_2CO_2)\cdot 2H_2O$ with Me = Cu, Zn]. The molecular and crystal structures of Cu(glu) and Zn(glu) have been reported,[12,13] and are peculiar among those of other CACS whose magnetic properties have been studied before. The copper ions are bonded by glu molecules forming polymeric chains

–glu–Cu–glu–Cu–glu–

being in addition connected by hydrogen bonds and carboxylate bridges, completing a three-dimensional magnetic network.

The main goal of this study of Cu(glu) is to determine the ability of a whole glutamic acid (glu) chain in providing for a superexchange interaction path between copper ions. The role of carboxylate and hydrogen bond bridges is also analyzed. The magnitudes of the corresponding exchange parameters $|J|$ are obtained from the angular variation of the width of the single exchange collapsed EPR line. A model based on Kubo and

(1) (a) Facultad de Bioquímica y Ciencias Biológicas. (b) Instituto de Desarrollo Tecnológico para la Industria Química (INTEC).
(2) Calvo, R.; Passeggi, M. C. G.; Novak, M. A.; Symko, O. G.; Oseroff, S. B.; Nascimento, O. R.; Terrile, M. C. *Phys. Rev. B* **1991**, *43*, 1074.
(3) (a) Calvo, R.; Mesa, M. A. *Phys. Rev. B* **1983**, *28*, 1244. (b) Calvo, R.; Mesa, M. A.; Oliva, G.; Zukerman-Schpector, J.; Nascimento, O. R.; Tovar, M.; Arce, R. *J. Chem. Phys.* **1984**, *81*, 4584. (c) Gennaro, A. M.; Levstein, P. R.; Steren, C. A.; Calvo, R. *Chem. Phys.* **1987**, *111*, 431. (d) Levstein, P. R.; Steren, C. A.; Gennaro, A. M.; Calvo, R. *Chem. Phys.* **1988**, *120*, 449. (e) Steren, C. A.; Gennaro, A. M.; Levstein, P. R.; Calvo, R. *J. Phys.: Condens. Matter* **1989**, *1*, 637.
(4) Newman, P. R.; Imes, J. L.; Cowen, J. A. *Phys. Rev. B* **1976**, *13*, 4093.
(5) Hoffmann, S. K.; Gozlar, J.; Sczepaniak, L. S. *Phys. Rev. B* **1988**, *37*, 7331.
(6) Wakamatsu, T.; Hashiguchi, T.; Nakano, M.; Sora, M.; Suga, H.; Zhi-Cheng, Tan. *Chin. Sci. Bull.* **1989**, *34*, 1795.
(7) (a) Calvo, R.; Siqueira, M. L.; Rapp, R. E. *Bull. Am. Phys. Soc.* **1992**, *37*, 655. (b) Siqueira, M. L.; Rapp, R. E.; Calvo, R. *Phys. Rev. B*, in press.
(8) Levstein, P. R.; Pastawski, H. M.; Calvo, R. *J. Phys.: Condens. Matter.* **1991**, *3*, 1877.
(9) Solomon, E. I.; Wilcox, D. E. In *Magneto-Structural Correlations in Exchange Coupled Systems*; Willet, R. D., Gatteschi, D., Khan, O., Eds.; D. Reidel: Dordrecht, Holland, 1985; p 463.
(10) Calvo, R.; Passeggi, M. C. G.; Isaacson, R. A.; Okamura, M. Y.; Feher, G. *Biophys. J.* **1990**, *58*, 149.
(11) Levstein, P. R.; Calvo, R. *Inorg. Chem.* **1989**, *29*, 1581.
(12) Gramaccioli, C. M.; Marsh, R. E. *Acta Crystallogr.* **1966**, *21*, 594.
(13) Gramaccioli, C. M. *Acta Crystallogr.* **1966**, *21*, 600.

0020-1669/93/1332-2078$04.00/0

Tomita's (KT) theory,[14,15] for the collapse of the resonances of the nonequivalent copper sites produced by the exchange interaction, is introduced to that aim.

We have also studied the EPR spectra of single crystals of Zn(glu) [isomorphous with Cu(glu)] doped with about 0.1% of ^{63}Cu, which replace substitutionally Zn atoms [Cu:Zn(glu)]. The information obtained in Cu:Zn(glu) is used to learn about the electronic properties of isolated copper ions, and to analyze the exchange collapsed EPR spectrum observed in Cu(glu).

Crystal Structures of Cu(glu) and Zn(glu)

The crystal structure of both Cu(glu)[12] and Zn(glu)[13] is orthorhombic, space group $P2_12_12_1$, with $Z = 4$. The lattice parameters for Cu(glu) [Zn(glu)] are $a = 11.084$ [11.190], $b = 10.350$ [10.463], and $c = 7.238$ [7.220] Å. The four symmetry-related molecules in the unit cell will be labeled as I, II, III, and IV. The Cu coordination in Cu(glu) (see Figure 1a) is approximately square planar, having two oxygens (O1–O3) from carboxylate groups of glu molecules glu^{I} and glu^{III} respectively, one amino nitrogen (N) belonging to glu^{I}, and one oxygen (Ow) from a water molecule, as equatorial ligands at about 1.99 Å. A fifth ligand at 2.299 Å, an oxygen (O2) from the carboxylate group of glu^{II}, and a sixth ligand (O4), from the same carboxylate group as O3, complete the distorted octahedron of ligands. As seen in Figure 1a, O4 is considerably displaced from the apical position, due to the rigidity of the carboxylate group (O4=C5—O3). The coordination around zinc ions in Zn(glu) (Figure 1b) is similar to that of copper ions in Cu(glu). In both compounds the ligands O1, O3, N, and Ow form the base of an approximately square pyramid with the O2 atom at the top. The copper ions in Cu(glu) are displaced downward by 0.15 Å from the center of the square base, while the zinc ions in Zn(glu) are similarly displaced by 0.32 Å, being approximately equidistant from all five atoms (Figure 1a,b).

The copper [zinc] ions in Cu(glu) [Zn(glu)] are bonded to the amino acid group of a glu molecule, and to the terminal carboxylate group of another glu (Figure 1a), forming chains along the **a** axis, which are called σ and σ' in Figure 2. The copper [zinc] ions are also connected by hydrogen bonds and carboxylate bridges (Figure 1a), forming copper [zinc] chains along the **c** axis, which are called C and C′ in Figure 2. The σ and σ' chains, as well as the C and C′ chains are symmetry related, and then chemically identical. Therefore, the copper [zinc] lattice in Cu(glu) [Zn(glu)] can be visualized as copper [zinc] ion chains along the **a** and **c** axes (Figure 2a) bonded between themselves, where the C and C′ chains are alternately connected to σ and σ' chains (Figure 2b), conforming the three-dimensional structure of the compounds. Copper ions are also connected by other weaker chemical bonds, which are unimportant for the transmission of the exchange interaction[11] and not analyzed here.

Experimental Section

Materials. Crystals of Cu(glu) were obtained at room temperature by slow evaporation from a saturated equimolar water solution of glutamic acid and basic copper carbonate. Crystals of Cu:Zn(glu) were obtained from a saturated water solution of glutamic acid, zinc chloride, and copper nitrate enriched 99% with the isotope ^{63}Cu, with a 0.1% Cu/Zn atomic ratio in the solution. This solution was adjusted to pH 5.3, and the crystallization done at 310 K. Prismatic crystals of Cu(glu) or Cu:Zn(glu) of about $2 \times 0.5 \times 0.5$ mm^3 were obtained in one week. The prisms are elongated along the direction of the **c** axis, and have (110) lateral faces. X-ray powder diffraction spectra proved that the materials obtained are equal to those reported in refs 12 and 13. The crystal axes **a** and **b** of the single-crystal samples were identified by measuring the angles between lateral faces with a goniometric microscope.

EPR Measurements. Measurements at 9.7 and 9.8 GHz were performed with a Bruker ER-200 EPR spectrometer, using a 12-in. rotating magnet, and a Bruker cylindrical cavity with 100-kHz field modulation. A Varian E-line spectrometer and a cylindrical cavity were used for the 33.3 GHz measurements. All of these experiments were carried out at room temperature. To orient the samples, a (110) face of the single crystals of Cu(glu) was glued to a cleaved KCl cubic holder, which defines a set **x**, **y**, **z** of orthogonal axes. The **c** axis is along the **z** axis of the holder, and **a** and **b** form angles $\alpha = 46.94°$ and $\epsilon = 136.94°$ with the **x** axis respectively (see inset in Figure 3). The sample holder was positioned in an horizontal plane at the top of a pedestal in the center of the microwave cavity, and the magnetic field **B** was rotated in the *xy*, *zx*, and *zy* planes of the samples. A single EPR line was observed in Cu(glu) for any orientation of **B**, at both microwave frequencies. The values for the squared gyromagnetic factor $g^2(\theta,\phi)$ measured at X-band, and the peak to peak line width $\Delta B_{pp}(\theta,\phi)$ at both bands are displayed

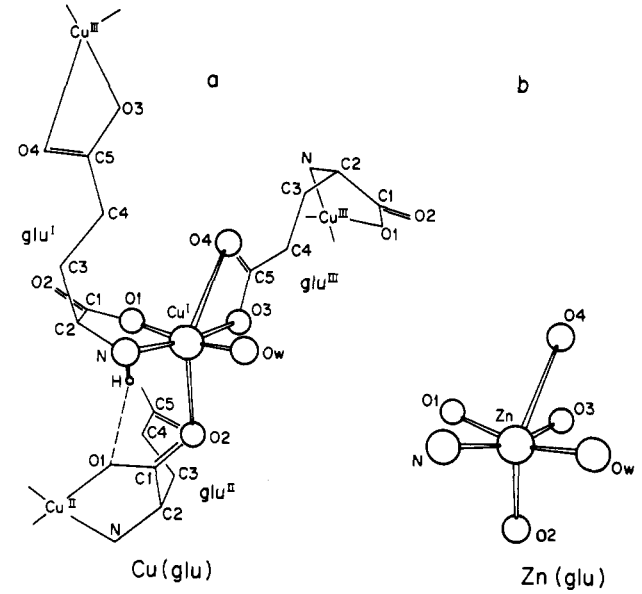

Figure 1. (a) Coordination around copper ions in Cu(glu). A copper ion at site I in the unit cell (Cu^{I}) is connected to two Cu^{III} by glu molecules (glu^{I} and glu^{III}) and to two Cu^{II} by carboxylate bridges and hydrogen bonds. The bond with the second Cu^{II} is omitted for clarity. Superscripts refer to the following transformation of the atomic coordinates: I = x, y, z; II = $0.5 - x, -y, 0.5 + z$; III = $0.5 + x, 0.5 - y, -z$; IV = $-x, 0.5 + y, 0.5 - z$. (b) Coordination around zinc ions in Zn(glu). The bonds between zinc ions are similar to those of copper ions in Cu(glu) and are omitted.

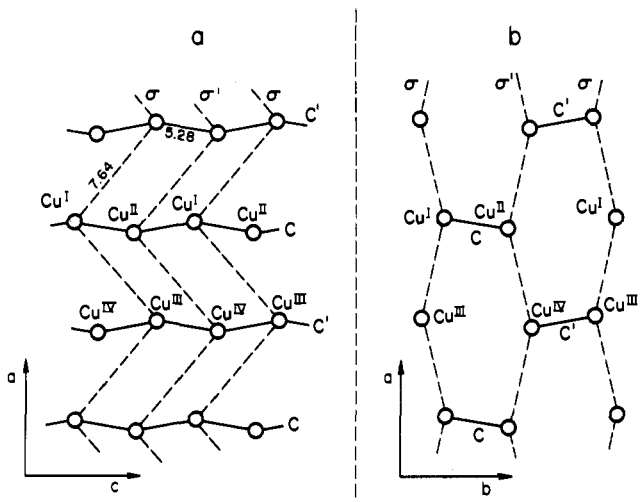

Figure 2. Orthogonal projection of the Cu(glu) crystal lattice on the *ca* and *ab* planes, showing a scheme of the exchange paths connecting copper ions. The distances are given in Å. The exchange paths in σ and σ' chains are glu molecules, and those in C and C′ chains are carboxylate bridges and hydrogen bonds.

(14) Kubo, R.; Tomita, K. *J. Phys. Soc. Jpn.* **1954**, *9*, 888.
(15) Yokota, M.; Koide, S. *J. Phys. Soc. Jpn.* **1954**, *9*, 953.

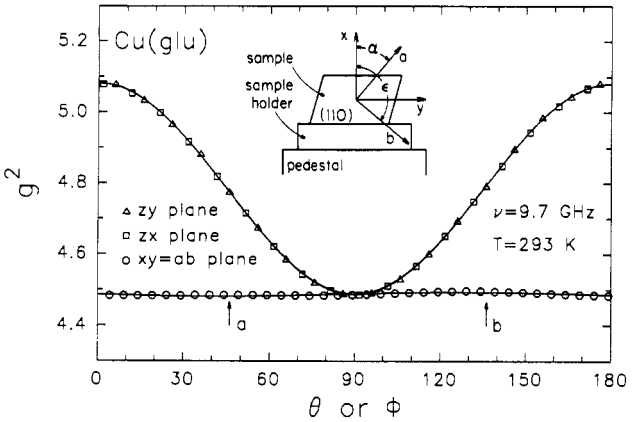

Figure 3. Angular variation of $g^2(\theta,\phi)$ at 9.7 GHz for the magnetic field applied in the *xy*, *zy*, and *zx* crystalline planes of the single crystal of Cu(glu). The inset shows the mounting of a sample of Cu(glu) on the measurement pedestal, indicating the positions of the crystalline axes **a** and **b** in the *xyz* system axes holder. The solid lines are obtained with the components of $\mathbf{g}^2$ given in Table II.

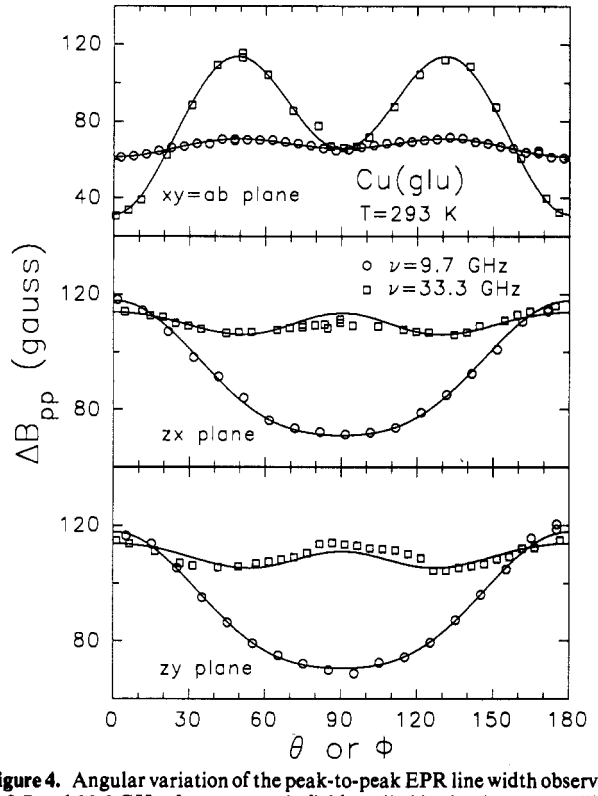

Figure 4. Angular variation of the peak-to-peak EPR line width observed at 9.7 and 33.3 GHz, for a magnetic field applied in the three crystalline planes *xy*, *zx*, and *zy* of a single crystal sample of Cu(glu). The solid lines are obtained with eq 17, and the parameters are included in Table III.

in Figures 3 and 4, respectively. The values of $g^2(\theta,\phi)$ obtained at 33.3 GHz are not shown because they are similar to those obtained at 9.7 GHz.

The Cu:Zn(glu) samples were glued to rexolite holders made according the crystallographic data of Zn(glu) (see inset in Figure 5). These holders allow us to orient accurately the samples and rotate the magnetic field **B** in the crystallographic planes *ab*, *ca*, and *cb*. There are four symmetry-related sites for copper ions in Cu(glu). However, in each crystallographic plane we observe only two groups of four resonance lines, belonging to the two pairs of copper sites which are nonequivalent in each plane.[16] The four lines splitting is due to the hyperfine coupling with the ^{63}Cu nucleus ($I = {}^3/_2$). A single four-lines spectrum was observed for **B** along **a**, **b**, and **c**. The positions in field of each resonance line were measured, and their values are displayed in Figure 5.

(16) Calvo, R.; Oseroff, S. B.; Abache, H. C. *J. Chem. Phys.* **1980**, *72*, 760.

Theory

Cu:Zn(glu). Noninteracting Spins. The observed EPR spectra in Cu:Zn(glu) can be explained with a spin Hamiltonian

$$\mathcal{H} = \mathcal{H}_z + \mathcal{H}_{hfs} = \beta\sum_{ip}\mathbf{S}_{ip}\cdot\mathbf{g}_i\cdot\mathbf{B} + \sum_{ip}\mathbf{S}_{ip}\cdot\mathbf{A}_i\cdot\mathbf{I}_{ip} \quad (1)$$

which includes Zeeman ($\mathcal{H}_z$) and hyperfine interactions ($\mathcal{H}_{hfs}$). In eq 1 $\mathbf{S}_{ip}$ and $\mathbf{I}_{ip}$ are the electronic and nuclear spins corresponding to the i-th copper site (i = I, ..., IV) in the *p*th unit cell ($S = {}^1/_2$, $I = {}^3/_2$). The sum in eq 1 is over the sites i, *p* in which copper ions replace zinc ions. **B** is the applied magnetic field, $\mathbf{g}_i$ and $\mathbf{A}_i$ are the electronic gyromagnetic and magnetic hyperfine tensors for copper ions in each site i, and β is the Bohr magneton. The energy levels of this spin Hamiltonian have been calculated up to second order by Weil,[17] whose results were used to analyze our experimental data. Superhyperfine terms are omitted in eq 1, because this structure was poorly resolved in our experiments.

Cu(glu). Interacting spins. The Hamiltonian of a system consisting of four magnetically non-equivalent interacting copper ions per unit cell is given by

$$\mathcal{H} = \mathcal{H}_z + \mathcal{H}_{ex} + \mathcal{H}_{dd} + \mathcal{H}_{hfs} + \mathcal{H}'' \quad (2)$$

where $\mathcal{H}_z$ and $\mathcal{H}_{hfs}$ are given in eq 1. In eq 2

$$\mathcal{H}_{ex} = {}^1/_2\sum_{pq,ij}J^{ij}_{pq}\mathbf{S}_{ip}\cdot\mathbf{S}_{jq};\ J^{ii}_{pp} = 0 \quad (3)$$

is the exchange interaction between copper spin pairs, which is assumed to be of Heisenberg type. $\mathcal{H}_{dd}$ is the magnetic dipolar interaction between copper ions, and $\mathcal{H}''$ involves other spin–spin interactions, as anisotropic and antisymmetric exchange. In systems where a single exchange-collapsed EPR line is observed, it is useful to separate $\mathcal{H}_z$ into two parts

$$\mathcal{H}_z = \beta\sum_{i=I,IV}\mathbf{S}_i\cdot\mathbf{g}_i\cdot\mathbf{B} = \beta\mathbf{S}\cdot\mathbf{g}\cdot\mathbf{B} + \beta\sum_{u=1,3}\mathbf{s}_u\cdot\mathbf{G}_u\cdot\mathbf{B} = \mathcal{H}^0{}_z + \mathcal{H}'_z \quad (4)$$

with

$$\mathbf{S}_i = \sum_p\mathbf{S}_{ip} \quad (5)$$

$$\mathbf{S} = \sum_{i=I,IV}\mathbf{S}_i \quad (6)$$

$$\mathbf{g} = {}^1/_4\sum_{i=I,IV}\mathbf{g}_i \quad (7)$$

and

$$\mathbf{s}_1 = -\mathbf{S}_I + \mathbf{S}_{II} + \mathbf{S}_{III} - \mathbf{S}_{IV}$$
$$\mathbf{G}_1 = {}^1/_4(-\mathbf{g}_I + \mathbf{g}_{II} + \mathbf{g}_{III} - \mathbf{g}_{IV}) \quad (8a)$$

$$\mathbf{s}_2 = \mathbf{S}_I - \mathbf{S}_{II} + \mathbf{S}_{III} - \mathbf{S}_{IV}$$
$$\mathbf{G}_2 = {}^1/_4(\mathbf{g}_I - \mathbf{g}_{II} + \mathbf{g}_{III} - \mathbf{g}_{IV}) \quad (8b)$$

$$\mathbf{s}_3 = \mathbf{S}_I + \mathbf{S}_{II} - \mathbf{S}_{III} - \mathbf{S}_{IV}$$
$$\mathbf{G}_3 = {}^1/_4(\mathbf{g}_I + \mathbf{g}_{II} - \mathbf{g}_{III} - \mathbf{g}_{IV}) \quad (8c)$$

The variables **S**, $\mathbf{s}_1$, $\mathbf{s}_2$ and $\mathbf{s}_3$ defined in eqs 5, 6, and 8 transform as irreducible representations of the point group D_2; e.g. s_z transforms as the representation B_1 and s_{1z}, s_{2z}, and s_{3z} transform as the representation B_2, B_3, and A_1, respectively.[18] As explained in the Appendix, these definitions simplify the line width calculations. The same situation applies for **g**, $\mathbf{G}_1$, $\mathbf{G}_2$, and $\mathbf{G}_3$, defined as linear combinations of the gyromagnetic tensors $\mathbf{g}_I$, $\mathbf{g}_{II}$, $\mathbf{g}_{III}$, and $\mathbf{g}_{IV}$ (eqs 7 and 8).

In eq 4 $\mathcal{H}^0{}_z$ is proportional to the total spin **S** and commutes with $\mathcal{H}_{ex}$ of eq 3. The "residual Zeeman interaction" $\mathcal{H}'_z$ arises

(17) Weil, J. A. *J. Magn. Reson.* **1975**, *18*, 113.
(18) Cotton, F. A. *Chemical Applications of Group Theory*; Interscience: New York, 1967.

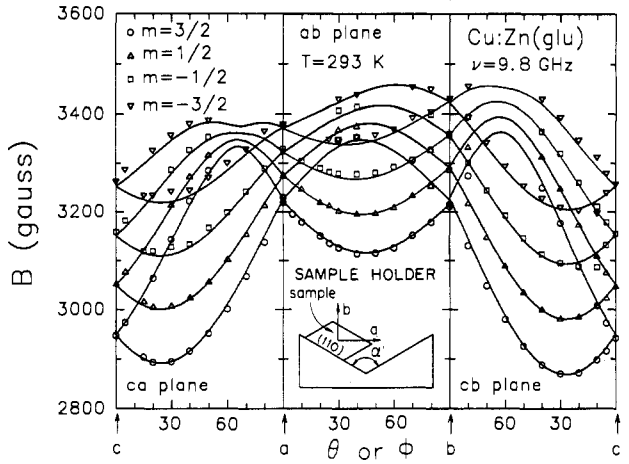

Figure 5. Angular variation of the position in field of each resonance line at 9.8 GHz and room temperature in Cu:Zn(glu). The solid lines were obtained fitting the experimental data using a least squares procedure as described in ref 16. The inset shows the rexolite holder having an angle $\alpha' = 93.8 \pm 0.8°$, which makes possible to orient accurately the sample with the magnetic field in the *ab*, *ca*, and *cb* crystalline planes.

from the nonequivalence of the four copper ions in the unit cell and does not commute with $\mathcal{H}^0_z$ and $\mathcal{H}_{ez}$. Since for Cu(glu), $\mathcal{H}'_z$, $\mathcal{H}_{dd}$, $\mathcal{H}_{hfs}$, and $\mathcal{H}''$ are smaller than $\mathcal{H}^0_z$ and $\mathcal{H}_{ex}$, we adopted a perturbative calculation to solve the problem. Equation 2 can be written as

$$\mathcal{H} = \mathcal{H}_0 + \mathcal{H}' \tag{9}$$

with

$$\mathcal{H}_0 = \mathcal{H}^0_z + \mathcal{H}_{ex} \tag{10}$$

and

$$\mathcal{H}' = \mathcal{H}'_z + \mathcal{H}_{dd} + \mathcal{H}_{hfs} + \mathcal{H}'' \tag{11}$$

Adopting the KT theory[14,19,20] for the calculation of the dynamical susceptibility, one ends up with a situation in which each term of $\mathcal{H}'$ (eq 11) is modulated by $\mathcal{H}_0$ (eq 10). In a zero-order approach the terms of $\mathcal{H}'$ are averaged out, and the EPR spectrum consists of a single line with the **g** tensor defined by eq 7. The modulation of $\mathcal{H}'$ by $\mathcal{H}_0$ modifies the EPR line widths.[14,19,20] In this work we are interested in the contribution of $\mathcal{H}'_z$ to $\Delta B_{pp}(\theta,\phi)$, which depends on magnetic field (or microwave frequency ω_0). As shown in the Appendix this contribution is proportional to ω_0^2, and is given by

$$\Delta B_{pp}(\theta,\phi) = \frac{\sqrt{\frac{2\pi}{3}}\omega_0^2\hbar}{g^3\beta}\sum_{u=1,3}\frac{[G_u(\theta,\phi)]^2}{\omega_u} \tag{12}$$

where

$$G_u(\theta,\phi) = \mathbf{h}\cdot\mathbf{G}_u\cdot\mathbf{h} \tag{13}$$

$\mathbf{h} = \mathbf{B}/|\mathbf{B}| = [\sin\theta\cos\phi, \sin\theta\sin\phi, \cos\theta]$ is the magnetic field orientation, and $\mathbf{G}_u$ is defined in eq 8, $g = {}^1/_3\mathrm{tr}(\mathbf{g})$ is the average value of the **g** tensor, and ω_u is the exchange frequency associated with each of the three terms of $\mathcal{H}'_z$ in eq 4. The relationship between ω_u and the exchange parameters J^{ij}_{pq}, defined in eq 3 for a lattice of four nonequivalent ions per unit cell, is also obtained in the Appendix. Considering only exchange interactions between nearest neighbor copper ions, we obtain

$$\omega_1^2 = 2\frac{(J_\sigma^2 + J_c^2)}{\hbar^2} \tag{14a}$$

$$\omega_2^2 = 2\frac{J_c^2}{\hbar^2} \tag{14b}$$

$$\omega_3^2 = 2\frac{J_\sigma^2}{\hbar^2} \tag{14c}$$

The exchange parameters J_σ and J_c in eq 14 correspond to pairs of copper ions connected by a glu molecule, or by carboxylate bridges and hydrogen bonds, respectively (see Figures 1a and 2). Other contributions to $\mathcal{H}'$ are not important for our purpose and are not analyzed here.

Analysis of the EPR Data

Cu:Zn(glu). The parameters of the spin Hamiltonian of eq 1 were obtained from the data using the perturbative formulas given by Weil[17] and a procedure described by Calvo et al.[16] The components of the second order tensors $\mathbf{g}_i^2$ and $\mathbf{A}_i^2$ were obtained in a first order approximation using a least squares procedure fitting the experimental values with the functions

$$g_i^2(\theta,\phi) = \mathbf{h}\cdot\mathbf{g}_i\cdot\mathbf{g}_i\cdot\mathbf{h} \tag{15}$$

$$g_i^2K_i^2(\theta,\phi) = \mathbf{h}\cdot\mathbf{g}_i\cdot\mathbf{A}_i\cdot\mathbf{A}_i\cdot\mathbf{g}_i\cdot\mathbf{h} \tag{16}$$

Second-order corrections to the positions of the resonance fields were considered as in refs 16 and 17, until agreement between experimental and calculated resonance positions were obtained. This was done with an electronic worksheet, which turned out to be very handy for this work, and the best fit is represented by solid lines in Figure 5. Note that this adjustment procedure produces a fairly good agreement to the data, although some small discrepancies occur in the high field region in Figure 5. The eigenvalues and eigenvectors of the gyromagnetic tensor $\mathbf{g}_i$ and the hyperfine tensor $\mathbf{A}_i$ for copper ions at site I are given in Table I. These show that $\mathbf{g}_i$ and $\mathbf{A}_i$ have coincident principal directions. The components of $\mathbf{g}_i$ and $\mathbf{A}_i$ for i = II, III, and IV can be obtained by applying the symmetry operations of the group D_2 to the components of the tensors corresponding to copper ions in site I. The experimental values for $g_i^2(\theta,\phi)$ and $g_i^2K_i^2(\theta,\phi)$ corresponding to site I are displayed in Figures 6 and 7.

Cu(glu). The Gyromagnetic Factor. The position of the single exchange collapsed resonance of the copper spins is described by $\mathcal{H}^0_z$ of eq 4. Since $g^2(\theta,\phi) = \mathbf{h}\cdot\mathbf{g}\cdot\mathbf{g}\cdot\mathbf{h}$, we calculated the components of $\mathbf{g}^2$ from the data at 9.7 and 33.3 GHz, using a least-squares procedure. These values are given in Table II, while solid lines in Figure 3 were obtained with the components of 9.7 GHz. The agreement between experimental and calculated values at 33.3 GHz was as good as that at 9.7 GHz. Table II shows that the tensor $\mathbf{g}^2$ is approximately diagonal and is axially symmetric at both bands. The axial symmetry of $\mathbf{g}^2$ (see Figure 3) is not expected from the crystallographic data. It can be understood from Figure 8, which displays the angular variation of $g_i^2(\theta,\phi)$ for each copper site in Cu:Zn(glu), and their average, together with the experimental values of $\mathbf{g}^2$ in Cu(glu). This average has an accidental axial symmetry, which explains the experimental results in Cu(glu).

Cu(glu). The EPR Line Width. The observed angular and frequency dependence of the line width (Figure 4) is well accounted by eq 12 plus three terms having second-order angular dependences, according to the crystal symmetry. The experimental values of $\Delta B_{pp}(\theta,\phi)$ at the two frequencies ω_0 shown in Figure 4, were

(19) Anderson, P. W.; Weiss, P. R. *Rev. Mod. Phys.* **1953**, *25*, 269. Anderson, P. W. *J. Phys. Soc. Jpn.* **1954**, *9*, 316.
(20) Bencini, A.; Gatteschi, D. *Electron Paramagnetic Resonance of Exchange Coupled Systems*; Springer: Berlin, 1989.

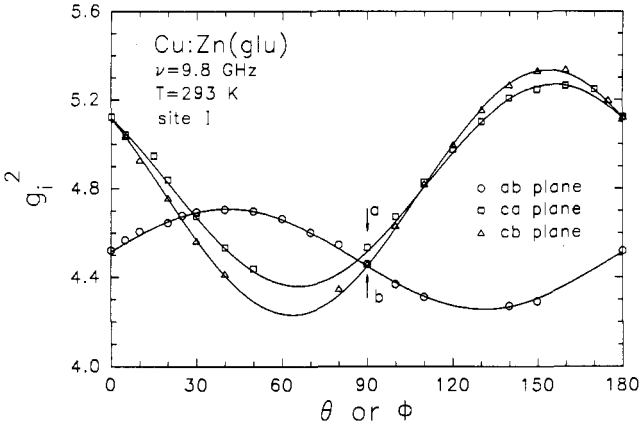

Figure 6. Angular variation of the squared gyromagnetic tensor $\mathbf{g}_i^2$ for copper ions at site I in the *ab*, *ca*, and *cb* planes of single crystals of Cu:Zn(glu). The solid lines were obtained with eq 15 and the parameters of Table I.

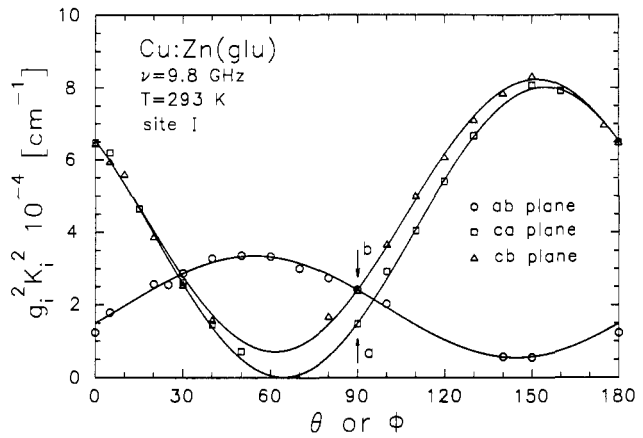

Figure 7. Angular variation of the $\mathbf{g}_i^2\mathbf{K}_i^2$ tensor for the copper ions at site I in the *ab*, *ca*, and *cb* planes of single crystals of Cu:Zn(glu). The solid lines were obtained with eq 16, and the parameters are given in Table I.

Table I. Eigenvalues and Eigenvectors of the Gyromagnetic Tensor $\mathbf{g}_i$ and the Hyperfine Structure Tensor $\mathbf{A}_i$ Corresponding to Copper Ions at Site I of the Unit Cell, Obtained at 9.8 GHz for ^{63}Cu in Cu:Zn(glu) with the Direction Cosines Referred to the Crystal Axes **a**, **b**, and **c**

eigenvalues	eigenvectors		
$g_1 = 2.053(3)$	−0.30(2)	0.897(4)	0.32(2)
$g_2 = 2.089(3)$	−0.875(9)	−0.12(2)	−0.47(1)
$g_3 = 2.345(3)$	−0.380(3)	−0.424(2)	0.822(1)
$A_1 = 39(1) \times 10^{-4}$ cm^{-1}	−0.34(4)	0.89(1)	0.31(2)
$A_2 = 1(1) \times 10^{-4}$ cm^{-1}	−0.86(2)	−0.16(2)	−0.48(1)
$A_3 = 131(1) \times 10^{-4}$ cm^{-1}	−0.383(4)	−0.427(5)	0.819(2)

fitted to the function

$$\Delta B_{pp}(\theta,\phi) = a_1 \sin^2\theta\cos^2\phi + a_2 \sin^2\theta \sin^2\phi + a_3 \cos^2\theta + \sum_{u=1,3} b_u [G_u(\theta,\phi)]^2 \quad (17)$$

where θ and ϕ give the orientation of the magnetic field in the **abc** crystal axes system. The functions $G_u(\theta,\phi)$, defined in eq 13, were calculated with the $\mathbf{g}_i$ tensors obtained in Cu:Zn(glu). The least-squares values of the parameters a_u and b_u ($u = 1, 2, 3$) are given in Table III, and predict the solid lines shown in Figure 4. Nonsecular terms arising from $\mathcal{H}'_z$ (see Appendix), having slightly different angular dependences than those included in eq 17, also add some minor contributions to the line width in the *zx* and *zy* planes. These may account for the small discrepancies to the fit shown in Figure 4.

The magnitudes of the coefficients a_u are a consequence of hyperfine and dipolar interactions, as well as antisymmetric and anisotropic exchange (see eq 11). They are not important for our purpose and will not be analyzed in detail. The decrease of a_1 with the increase of ω_0 can be related to nonsecular contributions to the line width.[21]

The functions $G_u(\theta,\phi)$ in eq 17 involve fourth-order as well as second-order angular contributions, which are not strictly orthogonal to the first three functions. This introduces an additional uncertainty on the values of the coefficients b_u not considered in those given in Table III, obtained from the dispersion of the fit.

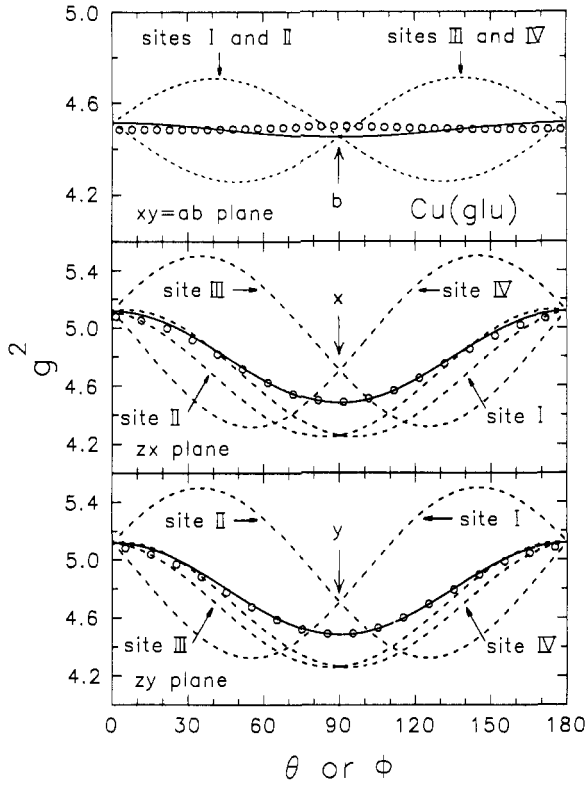

Figure 8. Angular variation of $\mathbf{g}_i^2$ for each copper site (dashed line) and their average (solid line) in the $xy = ab$, zx, and zy planes measured in single crystals of Cu(glu). The circles are the experimental data $[g^2(\theta,\phi)]$ at the X-band in Cu(glu). This figure shows the averaging effect of the exchange interaction, and how the axial symmetry of the overall $\mathbf{g}^2$ in Cu(glu) is achieved.

Table II. Components $(g^2)_{ij}$ of the Squared Gyromagnetic Tensor of Cu(glu) Obtained at 9.7 and 33.3 GHz[a]

	ν(GHz) = 9.7	ν(GHz) = 33.3
$(g^2)_{xx}$	4.486(1)	4.460(1)
$(g^2)_{yy}$	4.488(1)	4.460(1)
$(g^2)_{zz}$	5.081(1)	5.081(1)
$(g^2)_{xy}$	−0.006(1)	−0.007(1)
$(g^2)_{xz}$	0.000(1)	0.000(1)
$(g^2)_{yz}$	0.000(1)	0.000(1)

[a] They were calculated by least-squares fits of the function $g^2(\theta,\phi) = \mathbf{h}\cdot\mathbf{g}\cdot\mathbf{g}\cdot\mathbf{h}$ with the data, where $\mathbf{h} = \mathbf{B}/|\mathbf{B}|$ is the direction of the applied field.

Table III. Values of the Parameters a_u and b_u (in G) Obtained by Fitting Eq 17 with the Experimental values of the Line Width Measured at 9.7 and 33.3 GHz and Displayed in Figure 4

	ν(GHz) = 9.7	ν(GHz) = 33.3
a_1	61.4(6)	31(1)
a_2	65.7(6)	65(1)
a_3	117.8(6)	114(1)
b_1	$-14(7) \times 10^2$	$30(10) \times 10^2$
b_2	$-2(4) \times 10^2$	$7(7) \times 10^2$
b_3	$25.8(1.3) \times 10^2$	$231(3) \times 10^2$

(21) Gennaro, A. M.; Calvo, R. *J. Phys.: Condens. Matter.* **1989**, *1*, 7061; **1990**, *2*, 2873.

According to eq 12, the coefficients b_u are given by

$$b_u = \sqrt{\frac{2\pi}{3}} \frac{\hbar \omega_0^2}{\beta g^3 \omega_u} \quad (18)$$

As shown in Table III the coefficients b_u increase at 33.3 GHz, and the dependence of b_3 with ω_0 agrees well with the theory. From the value of b_3 at 33.3 GHz and using eq 18, we estimate $\omega_3 = 3.5 \times 10^{10}$ s^{-1}. Using this value and eq 14c, we obtain the exchange coupling constant $|J_\sigma| = 0.19 \pm 0.02$ K. The coefficients b_1 and b_2 are smaller than b_3, and their relative uncertainties are much larger. For that reason, it is not possible to prove the dependence on ω_0 predicted by eq 18. The negative signs of b_1 and b_2 at X-band can be attributed to nonsecular terms arising from antisymmetric exchange, as well as to antisymmetric terms from dipole–dipole interactions between nonequivalent anisotropic spins.[22] The value of b_1 at 33.3 GHz and eq 18 allow us to obtain $\omega_1 = 2.7 \times 10^{11}$ s^{-1}, which from eq 14a predicts the sum of the exchange coupling constants $(J_\sigma^2 + J_c^2)^{1/2} = 1.4 \pm 0.6$ K.

Discussion and Conclusions

The Gyromagnetic Factor. The results obtained for the gyromagnetic tensor in Cu:Zn(glu) are in agreement with those measured by Bonomo et al.[23] in ^{63}Cu:Cd(glu). This was expected since Zn(glu) and Cd(glu) are isostructural. The point symmetry at the copper [zinc] site in Cu(glu) [Zn(glu)] is C_1, but considering the arrangement of ligands around Cu in Cu(glu) [Zn in Zn(glu)] (see Figure 1), it may be approximated as C_s.[23] Then, the ground orbital state is a linear combination of the free ion orbitals $d(x^2-y^2)$, $d(zy)$, and $d(z^2)$. The eigenvalues for the gyromagnetic and hyperfine tensors of the copper ions obtained in Cu:Zn(glu) (see Table I), indicate that the main contribution to the ground state wave function is given by the $d(x^2 - y^2)$ orbital.[24]

The results obtained for the gyromagnetic tensor **g** in Cu(glu) (Table II) at both bands are very similar. The slight differences encountered may be attributed to small nonsecular contributions arising from $\mathcal{H}'$ (eq 11), which are not considered in our calculation. Also, a good agreement is obtained when the **g** tensor of Cu(glu) is compared with the average of the $\mathbf{g}_i$ tensors in Cu:Zn(glu) (see Figure 8). In Cu:Zn(glu), the largest value of $g^2(\theta,\phi)$ in the *ab* plane is along the **a** axis (see Figure 8), while the interactions between copper spins in Cu(glu) [not present in Cu:Zn(glu)] produce a value of $g^2(\theta,\phi)$ larger along the **b** axis than along **a**.

The EPR Line Width. Figure 4 shows a 180° periodicity for the line-width data at the X-band in the *zx* and *zy* planes. This contrasts with the 90° periodicity observed in the *xy* plane and suggests the presence of mutually competing mechanisms. Hyperfine, antisymmetric exchange, and contributions from either the dipolar or the anisotropic exchange interactions are able to produce the 180° periodicity. Other parts of the dipolar and anisotropic exchange, as well as the residual Zeeman interaction, can account for a 90° periodicity in the angular variation. The periodicity of the angular variation of the line width at 33.3 GHz in the *zx* and *zy* planes is different from the data at 9.7 GHz. This can be produced by nonsecular contributions, as well as by the enhancement due to the residual Zeeman interaction, because of the higher fields required. In the *xy* plane there is no change of the periodicity although a stronger variation is observed against the smooth dependences shown in the *zx* and *zy* plane. This indicates that the data in the *xy* plane provide information about the residual Zeeman interaction. However in this plane copper ions pairs I–II and III–IV are equivalent, and thus the strong exchange couplings between I–II and III–IV, become inoperative as far as its collapsing effect on the resonance is concerned. On the other hand the additional exchange interactions provided by the glutamic acid units still remain, and are able to collapse the lines as shown by the experiment. Then, the line width data at *Q* band in the $xy = ab$ plane provide the selectivity required to extract the value for J_σ.

From the line-width data at 33.3 GHz, we have evaluated the exchange parameters coupling nonequivalent copper ions using a model based in the KT theory.[14] This model allows us to obtain the absolute value of the exchange parameters J_{pq}^{ij} defined in eq 3, although no conclusion can be inferred about the magnetic ground state in Cu(glu). The value $|J_\sigma| = 0.19 \pm 0.02$ K obtained from the b_3 coefficient (eq 18), is related to the exchange interaction between coppers connected by a glu molecule (see Figures 1a and 2). The coefficient b_1 allows us to calculate $(J_\sigma^2 + J_c^2)$, and indicates $|J_c| > 1$ K. The chemical paths involving the exchange coupling constant J_c, are hydrogen bonds and carboxylate bridges (see Figures 1a and 2). Levstein and Calvo[11] have analyzed the correlation between the magnitudes of the exchange couplings and the exchange paths from EPR data in three similar CACS.[3c-e] They found that carboxylate groups involving a copper–apical oxygen (Cu–O_{ap}) bond, are more effective to transfer spin polarization that hydrogen bonds, and the magnitudes of exchange coupling constants are in these cases proportional to the inverse of the distance Cu–O_{ap}. The carboxylate bridges involved in Cu(glu) connect the copper ions with an apical oxygen O2 (see Figure 1a) at 2.299 Å. The value estimated from our line-width data $|J_c| > 1$ K, is in agreement with the proportionality given in ref 11, and indicates that the carboxylate bridges provide the important path for superexchange within C and C′ chains. Nevertheless, the uncertainties in the determination of J_c are large, reflecting that EPR methods are not appropriate for measurements of exchange interactions larger than 1 K. The coefficient b_2 have a small contribution to the line width in the planes measured, and no information can be obtained from its value.

We end up with a picture in which the dominant exchange interactions in Cu(glu) are those between copper ions connected by carboxylate bridges. Additional weaker exchange interactions exist between copper ions bridged by the σ skeleton of the glu molecules. Our results show how EPR allows us to evaluate these small exchange couplings in the presence of much larger couplings, a goal difficult to achieve with thermodynamic measurements as magnetic susceptibility or specific heat.

Acknowledgment. We are grateful to Prof. O. R. Nascimento in whose laboratory (IFQSC, USP, São Carlos, SP, Brazil) some of the data was taken. This work was supported by Grant 3-098600/88 of the Consejo Nacional de Investigaciones Científicas y Técnicas (CONICET), Argentina.

Appendix. Frequency-Dependent Contribution to the Line Width

In order to analyze the effect on the line width introduced by

$$\mathcal{H}'_z = \beta \sum_{u=1,3} \mathbf{s}_u \cdot \mathbf{G}_u \cdot \mathbf{B}$$

we performed a perturbative calculation using $\mathcal{H}_0$ (eq 10) as the unperturbed Hamiltonian, and $\mathcal{H}'_z$ as the perturbation. This is possible because the $\mathbf{G}_u$ tensors defined in eq 8 are small (small *g* anisotropies) and then $\mathcal{H} = \mathcal{H}_0 + \mathcal{H}'_z$ with $\mathcal{H}'_z \ll \mathcal{H}_0$. We chose $\zeta = \mathbf{g}\cdot\mathbf{h}/|\mathbf{g}\cdot\mathbf{h}|$ as the quantization axis. In this system $\mathcal{H}^0_z = \beta \mathbf{g} \mathbf{B} \mathbf{S}_\zeta$ and $\mathcal{H}_{ex}$ are diagonal. Then

$$\mathcal{H}'_z = \beta B \sum_{u=1,3} (\mathbf{G}_u \cdot \mathbf{h})_\zeta \mathbf{s}_{u\zeta} + \beta B \sum_{u=1,3} (\mathbf{G}_u \cdot \mathbf{h})_\perp \mathbf{s}_{u\perp}$$

where $\perp$ indicates the direction perpendicular to ζ. The first term in $\mathcal{H}'_z$ is diagonal and gives rise to secular contributions. The second term contains nonsecular contributions, which are

(22) Passeggi, M. C. G.; Calvo, R. *J. Magn. Reson.* **1989**, *81*, 378.
(23) Bonomo, R. P.; Pilbrow, J. R.; Sinclair, G. R. *J. Chem. Soc., Dalton Trans.* **1983**, 489.
(24) Zeiger, H. J.; Pratt, G. W. *Magnetic Interactions in Solids*; Oxford: London, 1973.

small, and will not be considered. The RF power absorbed by the sample $\chi''(\omega)$ is[20]

$$\chi''(\omega) = \frac{\omega V}{2KT}\langle M_{h'}M_{h'}\rangle \int_{-\infty}^{\infty} e^{-i\omega t}\,\zeta(t)\,dt \qquad (A1)$$

with

$$\zeta(t) = \frac{\langle M_{h'}(t)M_{h'}\rangle}{\langle M_{h'}M_{h'}\rangle}$$

where $M_{h'} = -\beta\mathbf{S}\cdot\mathbf{g}\cdot\mathbf{h}'$ is the component of the magnetic moment operator along the direction $\mathbf{h}' = \mathbf{B}_1/|\mathbf{B}_1|$ of the RF, V is the volume of the sample, and the angular brackets indicate the statistical average at the temperature T. Using the KT theory[14,20] up to second order, we obtain at $T = \infty$

$$\zeta(t) = e^{i\omega_0 t}\left[1 - \frac{\omega_0^2}{g^2(\theta,\phi)}\Gamma\cdot\mathbf{f}(t)\cdot\Gamma\right] \qquad (A2)$$

where $\mathbf{f}(t)$ is a tensor whose components are given by

$$f_{u,v}(t) = \int_0^t (t-\tau)\,\frac{\langle s_{u\zeta}^{ex}(\tau)s_{v\zeta}\rangle}{\langle S_\zeta^2\rangle}\,d\tau$$

and Γ is a vector with components $\Gamma_u = (\mathbf{G}_u\cdot\mathbf{h})_\zeta = \mathbf{h}\cdot\mathbf{g}\cdot\mathbf{G}_u\cdot\mathbf{h}/|\mathbf{g}\cdot\mathbf{h}|$. Since the components of the $\mathbf{s}_u$ defined in eq 8 transform like irreducible representations of the group D_2,[18] the nondiagonal components of $\mathbf{f}(t)$ are zero. Then, eq A2 is given by

$$\zeta(t) = e^{i\omega_0 t}\left[1 - \frac{\omega_0^2}{g^2(\theta,\phi)}\sum_{u=1,3}\Gamma_u^2 f_{u,u}(t)\right]$$

The simplest assumption for $\langle s_{u\zeta}^{ex}(\tau)s_{u\zeta}\rangle$ at high temperatures, is

$$\frac{\langle s_{u\zeta}^{ex}(\tau)s_{u\zeta}\rangle}{\langle S_\zeta^2\rangle} = \exp\left(-\frac{1}{2}\omega_u^2\tau^2\right) \qquad (A3)$$

where ω_u is the exchange frequency related to the exchange interaction. Replacing eq A3 in $f_{u,u}(t)$, we obtain

$$f_{u,u}(t) = \sqrt{\frac{\pi}{2}}\frac{t}{\omega_u}\,\mathrm{erf}\left(\frac{\omega_u t}{\sqrt{2}}\right) + \frac{\exp\left(-\frac{1}{2}\omega_u^2 t^2\right) - 1}{\omega_u^2}$$

where

$$\mathrm{erf}(x) = \frac{2}{\sqrt{\pi}}\int_0^x \exp(-t^2)\,dt$$

is the error function with $\mathrm{erf}(\infty) = 1$. Thus for the times of interest of $\zeta(t)$, eq A2 can be written as

$$\zeta(t) \approx e^{i\omega_0 t}\left(1 - \frac{\omega_0^2}{g^2(\theta,\phi)}\sum_{u=1,3}\sqrt{\frac{\pi}{2}}\Gamma_u^2\frac{t}{\omega_u}\right)$$

In the spirit of KT theory, we consider the terms within the brackets as the expansion of an exponential, arriving at

$$\zeta(t) \approx e^{i\omega_0 t}exp\left(-\frac{\omega_0^2}{g^2(\theta,\phi)}\sum_{u=1,3}\sqrt{\frac{\pi}{2}}\Gamma_u^2\frac{t}{\omega_u}\right)$$

Considering eq A1, this function predicts a Lorentzian line shape with a peak-to-peak line width proportional to the square of the microwave frequency ω_0.

$$\Delta B_{pp}(\theta,\phi) = \frac{\omega_0^2\hbar}{g^3(\theta,\phi)\beta}\sqrt{\frac{2\pi}{3}}\sum_{u=1,3}\frac{\Gamma_u^2}{\omega_u}\ \text{(in gauss)}$$

where $\Gamma_u \approx \mathbf{h}\cdot\mathbf{G}_u\cdot\mathbf{h}$ for Cu(glu).

Up to second order in $\mathcal{H}_{ex}$ the spin correlation function can be expanded as

$$\frac{\langle s_{u\zeta}^{ex}(\tau)s_{u\zeta}\rangle}{\langle S_\zeta^2\rangle} = 1 - \frac{\tau^2}{2\hbar^2}\frac{\langle[\mathcal{H}_{ex},(S_{I\zeta}+S_{IV\zeta})][(S_{I\zeta}+S_{IV\zeta}),\mathcal{H}_{ex}]\rangle}{\langle S_{I\zeta}^2\rangle}$$

where, I = I, II, and III for u = 1, 2, and 3, respectively. Therefore

$$\omega_1^2 = \frac{1}{2\hbar^2}\sum_p[(J_{op}^{I-II})^2 + (J_{op}^{I-III})^2 + (J_{op}^{II-IV})^2 + (J_{op}^{III-IV})^2]$$

$$\omega_2^2 = \frac{1}{2\hbar^2}\sum_p[(J_{op}^{I-II})^2 + (J_{op}^{II-III})^2 + (J_{op}^{I-IV})^2 + (J_{op}^{III-IV})^2]$$

$$\omega_3^2 = \frac{1}{2\hbar^2}\sum_p[(J_{op}^{I-III})^2 + (J_{op}^{II-III})^2 + (J_{op}^{I-IV})^2 + (J_{op}^{II-IV})^2]$$

where the index p sums over adjacent cells to the cell at the origin (p = 0).